Science Bulletin 63 (2018) 278–281

Contents lists available at ScienceDirect

Science Bulletin

journal homepage: www.elsevier.com/locate/scib

Short Communication

Secondary battery inspired α-nickel hydroxide as an efficient Ni-based heterogeneous catalyst for sulfate radical activation

Dongting Yue, Xufang Qian, Meng Ren, Mengyuan Fang, Jinping Jia, Yixin Zhao *

School of Environmental Science and Engineering, Shanghai Jiao Tong University, Shanghai 200240, China

ARTICLE INFO

Article history:
Received 4 January 2018
Received in revised form 14 January 2018
Accepted 18 January 2018
Available online 13 February 2018

Highly reactive radical species play an important role in synthetic chemistry, industrial processes, and environmental remediation applications [1,2]. The radicals can be formed by either thermal decomposition of highly active oxidants or by catalytic activation of stable oxidants under mild conditions [2]. Recently, the sulfate radical ($\cdot SO_4^-$) with its advantages of strong oxidizing power, selective reactivity, and stability over a broad range of pH has emerged as an excellent and versatile oxidant for a variety of application [3]. A wide range of persistent organic contaminants such as pharmaceutical waste, odor-causing compounds and pesticides can be effectively destroyed via sulfate radical-based advanced oxidation processes [4]. Sulfate radicals are usually generated catalytically by transition metal compounds and noble metals, especially well-known cobalt-based catalysts with considerably toxicity [5]. Ni is an abundant element with lower cost than Co and is well-known for its applications in homogeneous and heterogeneous catalytic reactions. However, the soluble Ni^{2+} ion and Ni metal-based catalysts have not been reported to be effective for sulfate radical activation. This inactivity may be due to the fact that the redox potential window of Ni/Ni^{2+} in aqueous solution is far lower than 1.92 V of Co^{2+}/Co^{3+} for the activation of sulfate radicals from peroxymonosulfate (PMS). Recently, earth abundant Ni-based heterogeneous catalysts, especially α-$Ni(OH)_2$, have achieved considerable success in electrochemical catalytic applications [6,7]. In these α-$Ni(OH)_2$-based electrochemical catalytic reactions, the Ni^{2+} in α-$Ni(OH)_2$ can be electrochemically oxidized to Ni^{3+} or even to the Ni^{4+} oxidation state for different catalytic applications [7]. Furthermore, the reversible Ni(III)/Ni(II) redox cycle based on $Ni(OH)_2 \leftrightarrow NiOOH$ has been utilized in rechargeable batteries with high stability in industrial applications over its long history [8,9]. Interestingly, the redox potential of $Ni(OH)_3/Ni^{2+}$ or $NiOOH/Ni(OH)_2$ in secondary battery could be higher up to 2.08 V. This redox potential would be enough to activate $S_2O_8^{2-}$ for the generation of $\cdot SO_4^-$ (redox potential of $S_2O_8^{2-}/SO_4^{2-}$ 2.0 eV). Here we for the first time to report using readily prepared α-$Ni(OH)_2$ nanosheets as an efficient catalyst for sulfate radical activation. The Ni(II) of α-$Ni(OH)_2$ can be reversibly and topochemically converted into Ni(III) in the form of NiOOH. These highly active sulfate radicals are sufficiently active for the degradation of persistent organic contaminants.

The α-$Ni(OH)_2$ sample was readily prepared via a simple hydrothermal synthesis and its X-ray diffraction (XRD) pattern is shown in Fig. 1a. The XRD pattern can be assigned as α-$Ni(OH)_2$ but it exhibits some mismatch with the standard α-$Ni(OH)_2$ XRD data (JCPDS No. 38-0715) as the (003) and (006) peaks are shifted ~0.25° and 0.5° to higher angle than the reference pattern. The smaller *c*-axis spacing evidenced by the positions of the (003) and (006) peaks can be attributed to different intercalated anions' size, which has also been observed in previous reports for hydrothermally prepared α-$Ni(OH)_2$ [8]. Scanning electron microscope (SEM) image of α-$Ni(OH)_2$ nanosheets was shown in Fig. 1b and hierarchical nanostructure of α-$Ni(OH)_2$ nanosheets was observed [10]. The transmission electron microscope (TEM) and high resolution TEM (HRTEM) images of α-$Ni(OH)_2$ nanosheets (Fig. 1c, d) illustrate their lateral dimensions and morphology. The α-$Ni(OH)_2$ sample consists of ultrathin nanosheets with a lateral size of 0.5–2.0 μm (Fig. 1c) and thicknesses below 10 m. The HRTEM image shows lattice fringes of the α-$Ni(OH)_2$ (012) and (002) plane with the *d*-spacing of 0.26 and 0.23 nm (Fig. 1d). The fast Fourier transform (FFT) pattern corresponding the red box in Fig. S1 (online) further illustrates the hexagonal symmetry of the α-$Ni(OH)_2$ nanosheets (insert in Fig. 1d). These materials characterization results confirm that our sample contains crystalline α-$Ni(OH)_2$ nanosheets, which provide high surface area for the catalytic reaction.

The Fenton-like catalytic performance of α-$Ni(OH)_2$ to generate sulfate radicals from peroxydisulfate (PDS) was evaluated by phe-

* Corresponding author.
E-mail address: yixin.zhao@sjtu.edu.cn (Y. Zhao).

https://doi.org/10.1016/j.scib.2018.02.002
2095-9273/

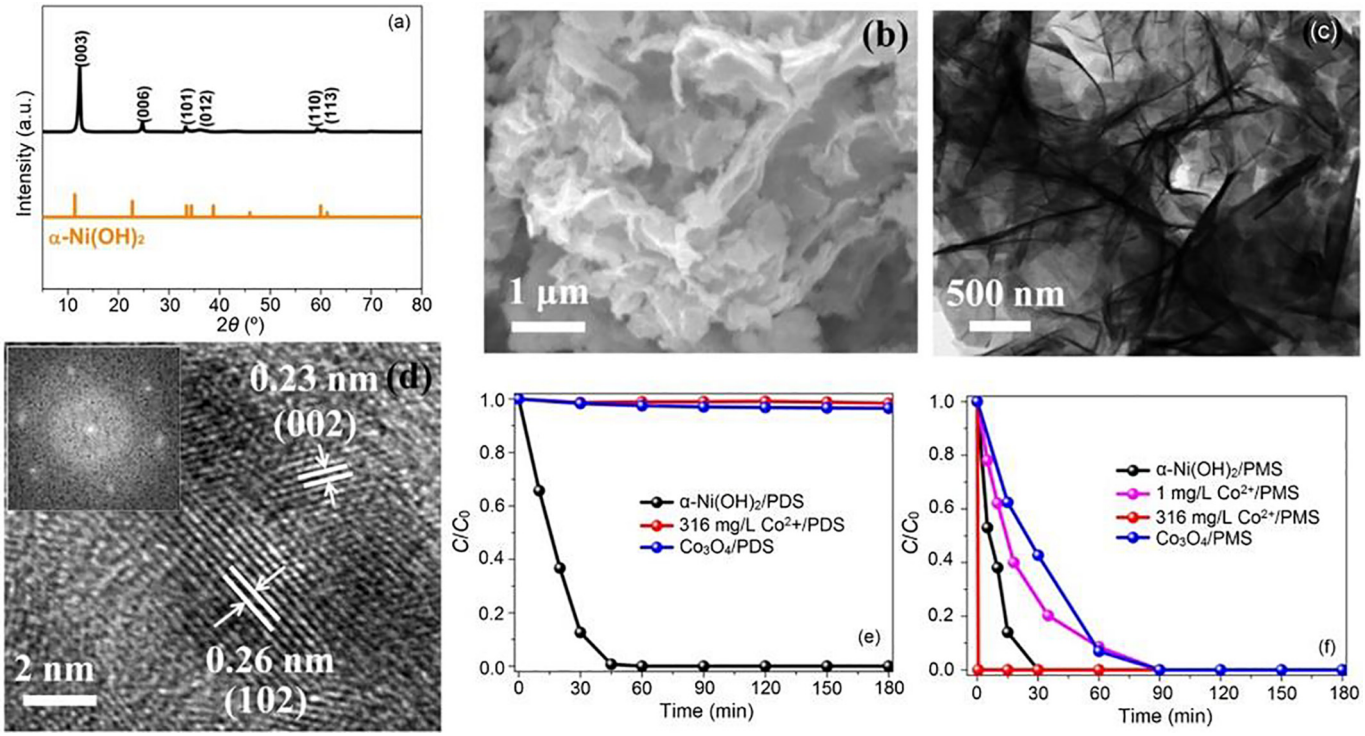

Fig. 1. (Color online) The material properties and environmental catalysis performance of α-$Ni(OH)_2$ nanosheets. (a) XRD pattern of as-prepared α-$Ni(OH)_2$ along with a simulated pattern. SEM (b), TEM (c), HRTEM images (d) and the corresponding FFT pattern (insert in Fig. 1d) for α-$Ni(OH)_2$ nanosheets. Phenol degradation activity of different catalysts in the presence of PDS (e) and PMS (f) (detailed experimental conditions are indicated in Supporting Information). Experimental conditions: [Phenol] = 50 mg/L, [PDS] = 0.4 g/L, [α-$Ni(OH)_2$] = 0.5 g/L (5.4 mmol/L), T = 298 K, and solution pH 10.0.

nol removal as in previous reports. Fenton-like reactions using PDS and α-$Ni(OH)_2$ nanosheets were examined under conditions similar to those of a previous report with some optimization. Phenol could not be degraded in the presence of only PDS or α-$Ni(OH)_2$ nanosheets (Fig. S2 online). With both α-$Ni(OH)_2$ and PDS present, phenol removal becomes fast and efficient. The degradation of phenol was analyzed by the time-dependent evolution of the high performance liquid chromatography (HPLC) (Fig. S3 online). Phenol was found to be degraded completely. However, some small peaks attributed to organic acids such as acetic acid appear along with the disappearance of phenol. Accordingly, we postulate that most of the phenol is been mineralized to CO_2 in the Fenton-like reaction but a small fraction is decomposed to small, oxidized organic compounds (Fig. S3 online). We further optimized the heterogeneous Fenton-like reaction by investigating other factors such as the solution pH and the amount of PDS, monitoring their effect on the phenol degradation efficiency (Fig. S4 online). Under the optimized conditions, α-$Ni(OH)_2$ exhibits excellent activity for phenol degradation by PDS activation.

The Co ion and Co based metal oxides have been identified as the most efficient low-cost sulfate radical generation catalysts [5]. However, both the Co^{2+} ion and Co_3O_4 nanoparticles with the same molar amounts of Co as in the α-$Ni(OH)_2$ samples studied showed no detectable catalytic activity for PDS decomposition of phenol (Fig. 1e). The inactivity of Co-based catalysts for PDS activation is consistent with an earlier study [3,5]. Most reported studies of Co-based Fenton-like catalysts have been evaluated using PMS, which is easier to activate than PDS. Here we compared our α-$Ni(OH)_2$ nanosheet sample with both Co^{2+} ions and commercially available Co_3O_4 nanoparticles. The Co_3O_4 nanoparticles had similar or even larger Brunauer-Emmett-Teller (BET) surface areas than our α-$Ni(OH)_2$ nanosheet samples (Fig. S5 online). As shown in Fig. 1f, the Co^{2+}/PMS homogeneous system with 316 mg/L Co^{2+} (or 5.36 mmol/L Co^{2+}) had very high reactivity and 100% of the phenol was decomposed in less than 1 min. But this high Co^{2+} concentration greatly exceeds the <1 ppm (1 ppm = 1 mg/L) environmental safety standard. At Co^{2+} concentrations lower than 1 ppm, the Fenton-like decomposition reaction rate decreased dramatically and it took 90 min to completely remove phenol. In the case of Co_3O_4 nanoparticles, phenol removal reached 94% within 60 min, which is comparable to the activity of 1 ppm Co^{2+} ion. Interestingly, α-$Ni(OH)_2$ can catalyze the Fenton-like reaction to degrade phenol almost quantitatively within 30 min. Furthermore, the Ni leaching level after the reaction was found to be <0.1 ppm when using α-$Ni(OH)_2$ as the Fenton-like catalyst (Table S1 online).

These results demonstrated that α-$Ni(OH)_2$ is even better than the state-of-the-art sulfate radical activator of Co_3O_4 nanoparticles as a PMS Fenton-like catalyst. Most previously reported sulphate activator catalysts are only active with either PMS or PDS. In contrast, α-$Ni(OH)_2$ nanosheets can serve as an efficient and general catalyst to activate both PMS and PDS for phenol removal with high activity. To reveal the excellent stability of α-$Ni(OH)_2$ further, amorphous-$Ni(OH)_2$ was prepared for comparison. α-$Ni(OH)_2$ nanosheets show almost the same catalytic activity for the decomposition of phenol after four cycles and even after pretreated by excess PDS (Figs. S6 and S7 online). For the amorphous $Ni(OH)_2$, the removal efficiency of phenol drops quickly from 100% to 13% after four cycles, indicative of poor catalyst stability (Fig. S8 online). To further evaluate the extent of mineralization of phenol using the α-$Ni(OH)_2$ nanosheet catalyst, the TOC removal efficiency was also monitored. Fig. S9 (online) shows that the TOC removal of phenol was more than 90%, implying high mineralization activity of α-$Ni(OH)_2$ as a Fenton-like catalysts for organic pollutant degradation. The α-$Ni(OH)_2$ samples all show <0.1 ppm Ni leaching in

four cycle reactions (Table S1 online). This residue content from α-$Ni(OH)_2$ samples after each cycle is lower than the 1 ppm Ni limitation regulated in the EU and the US. These results indicated that α-$Ni(OH)_2$ nanosheet catalyst is an efficient, low toxicity and stable catalyst for sulfate radical generation by activation of both PDS and PMS in the Fenton-like reaction.

Although α-$Ni(OH)_2$ exhibits very low Ni leaching, we still need to exclude the possible catalytic effect of dissolved Ni ions. To further understanding the role and mechanism of α-$Ni(OH)_2$ for the activation of PDS, Ni powder and soluble Ni^{2+} compounds were also investigated under neutral conditions. As shown in Fig. 2a, phenol could not be degraded by using Ni powder or Ni^{2+} ions with PDS whereas α-$Ni(OH)_2$ nanosheets exhibited efficient phenol removal under the same condition. Neither Ni powder nor Ni^{2+} ion is able to work for PMS activation. This observation is consistent with previous findings of the inactivity of Ni for sulfate radical activation[5]. Based on this result, we could exclude the possibility that α-$Ni(OH)_2$ acts simply as a source of Ni^{2+} ions or Ni. Consequently, we can ascribe the Fenton-like activities to the unique properties of α-$Ni(OH)_2$. To explore the mechanism of the α-$Ni(OH)_2$ activation of PDS, we first employed spin-trapping electron paramagnetic resonance (EPR) analysis to identify the short-lived radicals generated at different pH values. First, the EPR data confirmed the formation of radicals in presence of α-$Ni(OH)_2$ and PDS. Secondly, Fig. 2b revealed that the relative EPR signals intensity decreases at lower pH, which is consistent with the removal activity of phenol at different pH values shown in Fig. S4a (online).

Based on these observations, we propose the sulfate radical activation mechanism via α-$Ni(OH)_2$ from PDS shown in Fig. 2c. Some of Ni(II) in α-$Ni(OH)_2$ can be oxidized to Ni(III), which has been known and even used to prepare NiOOH by oxidizing amorphous $Ni(OH)_2$ with concentrated PDS in highly basic solution. This oxidation process might have a redox potential similar to Co^{2+}/Co^{3+} or Ag/Ag^+, thereby inducing or activating the formation of the $\cdot SO_4^-$ radical intermediate (Eq. (1)) [9,11]. Additionally, it could also lead to the formation of HO· radicals under alkaline conditions (Eq. (2)). The $\cdot SO_4^-$ radical and HO· radicals, as a powerful oxidizing agent [3], can oxidize phenol effectively. Subsequently, the Ni(III) sites of NiOOH can be reduced to Ni(II) as $Ni(OH)_2$ at a similar potential as the Co^{3+}/Co^{2+} or Ag^+/Ag couples that facilitate the formation of $\cdot S_2O_8^-$ from PDS. These highly active $\cdot S_2O_8^-$ radicals can react directly with phenol or be further converted into $\cdot SO_4^-$ radicals for phenol removal (Eqs. (3) and (4)) via the Fenton-like reaction [3]. Of course, the Fenton-like catalytic reaction rates via the redox couples Ni(II)/Ni(III) and Ni(III)/Ni(II) could be different. We hypothesize that the redox cycle between $Ni(OH)_2$ and NiOOH can finally reach an equilibrium to activate PDS to form $\cdot SO_4^-$ radicals and/or $\cdot S_2O_8^-$ radicals to degrade the organic pollutant.

$$Ni(II)+S_2O_8^{2-} \rightarrow Ni(III)+SO_4^{2-}+\cdot SO_4^- \quad (1)$$

$$\cdot SO_4^- + H_2O \rightarrow SO_4^{2-}+H^+ +\cdot OH \quad (2)$$

$$Ni(III)+S_2O_8^{2-} \rightarrow Ni(II)+\cdot S_2O_8^- \quad (3)$$

$$\cdot S_2O_8^- + SO_4^{2-} \rightarrow \cdot SO_4^- +\cdot S_2O_8^{2-} \quad (4)$$

In above mechanism, the surface or partial Ni(II) sites on α-$Ni(OH)_2$ would be oxidized to Ni(III) sites after the Fenton-like reaction. XPS characterization was carried out to explore changes in α-$Ni(OH)_2$ before and after the PDS activation reaction (Fig. 2d). The Ni $2p_{3/2}$ XPS peaks with binding energy of 855.8 eV for fresh α-$Ni(OH)_2$ samples could be assigned to Ni^{2+}. After the Fenton-like reaction for phenol removal, the binding energy of Ni $2p_{3/2}$ XPS peaks was shifted positively to 856.5 eV, which could be related to the

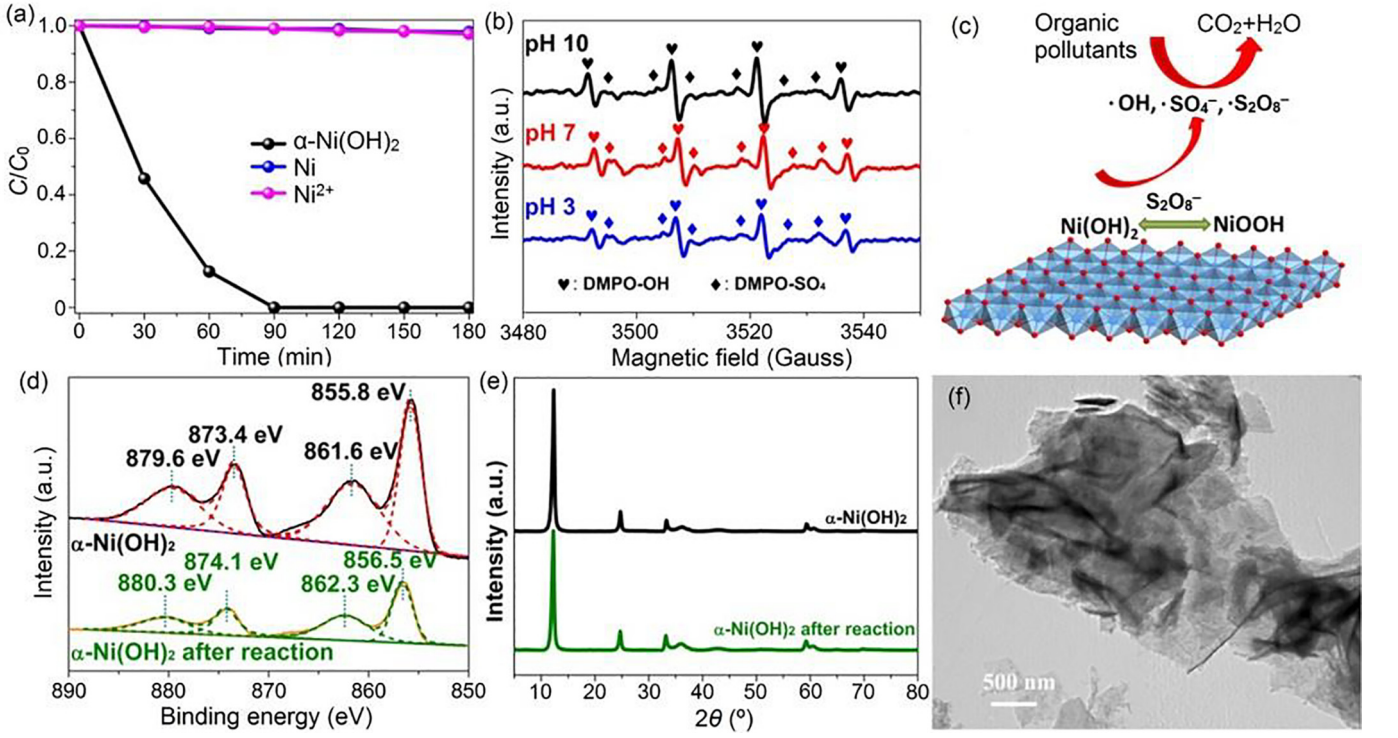

Fig. 2. (Color online) The reaction mechanism of α-$Ni(OH)_2$ nanosheets for sulfate radical activation. (a) Effect of different catalysts for the catalysis of PDS and the degradation of phenol. Experimental conditions: [Phenol] = 50 mg/L, [PDS] = 0.4 g/L, 5.4 mmol/L of α-$Ni(OH)_2$, 5.4 mmol/L Ni powder and 1 ppm Ni^{2+}, T = 298 K, solution pH at 7.0. (b) 5,5-Dimethylpyrroline-oxide (DMPO) spin-trapping EPR spectra at different pH. (c) Schematic illustration of the Fenton-like phenol degradation mechanism in the α-$Ni(OH)_2$/PDS system. (d) High-resolution XPS spectrum of Ni 2p of α-$Ni(OH)_2$ nanosheets before and after reaction. (e) XRD patterns for as-prepared α-$Ni(OH)_2$ before and after reaction. (f) TEM image taken of α-$Ni(OH)_2$ samples after 4 runs.

formation of Ni^{3+} after the partial oxidation of α-$Ni(OH)_2$. Interestingly, the light green α-$Ni(OH)_2$ powder also changes to black after the Fenton-like reaction (Fig. S10 online). This color change is similar to previous the change in α-$Ni(OH)_2$ after electrochemical water oxidization reaction due to the formation of higher oxidation states of Ni. All these results suggest the formation of Ni^{3+} sites in α-$Ni(OH)_2$ after the Fenton-like reaction [8,11]. Although the XPS results showed the formation of Ni^{3+}, the α-$Ni(OH)_2$ samples did not exhibit any observable $Ni(OH)_2 \leftrightarrow NiOOH$ phase change in their XRD patterns. The Ni(III) molar ratio in the α-$Ni(OH)_2$ samples was additionally measured by titration as shown in Table S2 (online). The Ni(III) molar ratios are all relatively low after different cycles of the Fenton-like reaction, and the Ni(III) content is almost the independent of the number of Fenton-like reaction cycles. These results confirm our proposed mechanism of Fenton-like activation of $\cdot SO_4^-$ radicals via reversible $Ni(II) \leftrightarrow Ni(III)$ redox cycles based on the $Ni(OH)_2 \leftrightarrow NiOOH$ reaction.

The well-known reversible $Ni(OH)_2 \leftrightarrow NiOOH$ reaction might be the mechanism behind the high stability of the catalyst. To obtain a more detailed understanding and confirmation of the relatively high stability of α-$Ni(OH)_2$ from view of material properties, XRD and TEM analysis were carried out before and after the Fenton-like reaction. Fig. 2e illustrated that α-$Ni(OH)_2$ samples after 4 reaction cycles maintained morphology, lattice parameters and crystallinity similar to those of fresh samples shown in Fig. 1a. There is no obvious morphology change from TEM and HRTEM images (Fig. 2f and S11 online). The XRD patterns of α-$Ni(OH)_2$ before and after reaction were identical, demonstrating the phase stability of α-$Ni(OH)_2$. These material characterization results reveal the high material stability of α-$Ni(OH)_2$, which is consistent with its well-known electrochemical applications. From these observations we can conclude that crystalline α-$Ni(OH)_2$ has high material stability which helps to prevent nickel leaching and thus makes α-$Ni(OH)_2$ environmentally friendly as a catalysts for Fenton-like reaction.

In summary, we for the first time demonstrate a Ni-based Fenton-like catalyst for sulfate radical generation. Hydrothermally prepared α-$Ni(OH)_2$ nanosheets can serve as an efficient Fenton-like catalyst to activate both PMS as well as less reactive PDS to generate sulfate radicals, exceeding that of the state-of-the-art Co_3O_4 nanoparticle catalysts. This superior performance can be ascribed to the efficient reversible Ni^{2+}/Ni^{3+} redox cycle in α-$Ni(OH)_2$. α-$Ni(OH)_2$ shows high material stability and exhibits low Ni leaching after the Fenton-like catalytic reaction. This finding, based on the well-known secondary battery material of α-$Ni(OH)_2$ with its efficient redox cycling, may be promising for extension to other secondary battery material as potential catalyst candidates for use in radical activation applications.

Conflict of interest

The authors declare that they have no conflict of interest.

Acknowledgments

This work was supported by the National Natural Science Foundation of China (21777096 and 21777097) and the China Postdoctoral Science Foundation (2017M621483).

Appendix A. Supplementary data

Supplementary data associated with this article can be found, in the online version, at https://doi.org/10.1016/j.scib.2018.02.002.

References

[1] Recupero F, Punta C. Free radical functionalization of organic compounds catalyzed by *n*-hydroxyphthalimide. Chem Rev 2007;107:3800–42.
[2] Gligorovski S, Strekowski R, Barbati S, et al. Environmental implications of hydroxyl radicals (·OH). Chem Rev 2015;115:13051–92.
[3] Liu H, Bruton TA, Doyle FM, et al. In situ chemical oxidation of contaminated groundwater by persulfate: decomposition by Fe(III)- and Mn(IV)-containing oxides and aquifer materials. Environ Sci Technol 2014;48:10330–6.
[4] Kronholm J, Riekkola ML. Potassium persulfate as oxidant in pressurized hot water. Environ Sci Technol 1999;33:2095–9.
[5] George PA, Dionysios DD. Radical generation by the interaction of transition metals with common oxidants. Environ Sci Technol 2004;38:3705–12.
[6] Simon T, Bouchonville N, Berr MJ, et al. Redox shuttle mechanism enhances photocatalytic H_2 generation on Ni-decorated cds nanorods. Nat Mater 2014;13:1013–8.
[7] Long X, Li G, Wang Z, et al. Metallic iron-nickel sulfide ultrathin nanosheets as a highly active electrocatalyst for hydrogen evolution reaction in acidic media. J Am Chem Soc 2015;137:11900–3.
[8] Gao M, Sheng W, Zhuang Z, et al. Efficient water oxidation using nanostructured alpha-nickel-hydroxide as an electrocatalyst. J Am Chem Soc 2014;136:7077–84.
[9] Oliva P, Leonardi J, Laurent JF, et al. Review of the structure and the electrochemistry of nickel hydroxides and oxy-hydroxides. J Power Sources 1982;8:229–55.
[10] Guan J, Liu L, Xu L, et al. Nickel flower-like nanostructures composed of nanoplates: one-pot synthesis, stepwise growth mechanism and enhanced ferromagnetic properties. CrystEngComm 2011;13:2636.
[11] Fu XZ, Zhu YJ, Xu QC, et al. Nickel oxyhydroxides with various oxidation states prepared by chemical oxidation of spherical β-$Ni(OH)_2$. Solid State Ionics 2007;178:987–93.